Estuarine, Coastal and Shelf Science 186 (2017) 100–111

Contents lists available at ScienceDirect

Estuarine, Coastal and Shelf Science

journal homepage: www.elsevier.com/locate/ecss

Carbon-13 labelling shows no effect of ocean acidification on carbon transfer in Mediterranean plankton communities

L. Maugendre [a, b, *], J.-P. Gattuso [a, b, c], A. de Kluijver [d], K. Soetaert [e], D. van Oevelen [e], J.J. Middelburg [f], F. Gazeau [a, b]

[a] Sorbonne Universités, UPMC Univ Paris 06, UMR 7093, LOV, Observatoire Océanologique de Villefranche, 06230 Villefranche-sur-Mer, France
[b] CNRS-INSU, UMR 7093, Laboratoire d'Océanographie de Villefranche, 06230 Villefranche-sur-Mer, France
[c] Institute for Sustainable Development and International Relations (IDDRI), Sciences Po, 27 rue Saint Guillaume, F-75007 Paris, France
[d] Deltares, Delft, The Netherlands
[e] Department of Ecosystems Studies, Royal Netherlands Institute for Sea Research (NIOZ), Yerseke, The Netherlands
[f] Department of Earth Sciences, Faculty of Geosciences, Utrecht University, The Netherlands

ARTICLE INFO

Article history:
Received 30 March 2015
Received in revised form
15 December 2015
Accepted 17 December 2015
Available online 22 December 2015

Keywords:
Ocean acidification
Plankton communities
Carbon transfer
^{13}C and biomarkers
Mesocosm experiments
Mediterranean Sea

ABSTRACT

Despite an increasing number of experiments, no consensus has emerged on the effect of ocean acidification on plankton communities and carbon flow. During two experiments, performed in the Bay of Calvi (France, Corsica; summer 2012) and the Bay of Villefranche (France; winter 2013), nine off-shore mesocosms (~50 m^3) were deployed among which three served as controls and six were enriched with CO_2 to reach partial pressure of CO_2 (pCO_2) levels from 450 to 1350 µatm and 350–1250 µatm in the Bay of Calvi and the Bay of Villefranche, respectively. In each mesocosm, inorganic ^{13}C was added in order to follow carbon transfer from inorganic via bulk particulate organic carbon and phytoplankton to bacteria by means of biomarkers as well as to zooplankton and settling particles. Despite very low plankton biomasses, labelled carbon was clearly transferred through plankton communities. Incorporation rates in the various plankton compartments suggested a slow-growing community based on regenerated production in the Bay of Calvi while in the Bay of Villefranche, fast-growing species were clearly dominating community production at the start with a shift toward slow-growing species during the experiment due to nutrient limitation. Both bulk and group-specific productions rates did not respond to increasing pCO_2 levels. These experiments were the first conducted in the Mediterranean Sea under low nutrient concentrations and phytoplankton biomasses and suggest that ocean acidification may not significantly impact plankton carbon flows in low nutrient low chlorophyll (LNLC) areas.

1. Introduction

The ocean is the largest active reservoir of carbon on Earth, absorbs about 2.6 ± 0.5 Pg C yr^{-1} (Le Quéré et al., 2014) and has a key role in regulating carbon flow on Earth. Carbon dioxide (CO_2) fluxes from the atmosphere to the ocean are partly controlled by primary production, community respiration and organic matter (OM) export to the deep-sea, the so-called biological pump. Primary production rates in the surface layer depend on environmental conditions such as temperature, water-column structure (mixed *vs.* stratified), irradiance levels and nutrient availability. The freshly produced OM can be consumed by zooplankton or exported to the deep-sea but a large fraction is respired and degraded by heterotrophic bacteria in the upper layer producing CO_2 as well as recycled inorganic nutrients brought back in the ecosystem (Rivkin and Legendre, 2001). The CO_2 equilibrium between atmosphere and ocean is then dependent on the trophic status and metabolic state of surface plankton communities.

Over the last century, CO_2 concentration in the atmosphere has increased at an unprecedented rate in the Earth's history due to human activities, warming the lower atmosphere and the ocean. Furthermore, 26% of the emitted CO_2 dissolves in seawater (Le Quéré et al., 2014) causing an acidification of the ocean with potential effects on plankton metabolic rates in the upper layer (Riebesell and Tortell, 2011). Dissolved CO_2 is the main substrate for

* Corresponding author. Sorbonne Universités, UPMC Univ Paris 06, UMR 7093, LOV, Observatoire Océanologique de Villefranche, 06230 Villefranche-sur-Mer, France.
E-mail address: laure.maugendre@gmail.com (L. Maugendre).

http://dx.doi.org/10.1016/j.ecss.2015.12.018
0272-7714/

photosynthesis but the activity of the RuBisCO, the enzyme necessary for carbon fixation, is suboptimal at CO_2 concentrations present in ocean surface waters (Reinfelder, 2011). Therefore, primary production rates might increase under elevated CO_2 levels resulting in carbon overconsumption relative to other nutrients (Riebesell et al., 2007). This could further alter phytoplankton-derived dissolved organic matter (DOM) production and composition (Engel et al., 2004; Riebesell et al., 2007), and consequently increase bacterial carbon consumption as DOM is the main substrate for their growth (Grossart et al., 2006). In parallel, the formation of C-rich aggregates could also increase carbon export and therefore the efficiency of the biological pump (Engel et al., 2004). Furthermore, due to differences in carbon fixation pathways between phytoplankton species, carbon export capacities of the surface ocean could be altered due to modifications of phytoplankton community size structure and sinking capacities (Klaas and Archer, 2002). An significant number of experiments have assessed the effects of ocean acidification on plankton composition and functioning. These studies provided variable and sometimes conflicting results, preventing the development of a general concept on the effects of ocean acidification (see Riebesell and Tortell, 2011 for review). For instance, in some studies, ocean acidification has been shown to modify the community structure towards more diatoms (Tortell et al., 2008, 2002) or towards smaller species (Brussaard et al., 2013). In other studies, no changes were found (Nielsen et al., 2010, 2012).

As the functioning of plankton communities depends on many ecological interactions between biotic and abiotic compartments, there is a strong need to study natural assemblages rather than individual species or strains. Carbon flow within natural plankton communities has been studied using stable isotopes labelling coupled with biomarkers (Middelburg et al., 2000; van den Meersche et al., 2011). The addition of ^{13}C dissolved inorganic carbon and subsequent transfer to phytoplankton, heterotrophic bacteria as well as zooplankton and sinking particles, allows following carbon transfer through plankton communities. The estimation of carbon incorporation in various taxonomic groups can be performed through the analysis of ^{13}C enrichment in phospholipids derived fatty acids (PLFA) biomarkers. PLFA are cell membrane components, produced by phytoplankton and heterotrophic bacteria, which occur in relatively fixed proportion in cells and allow distinguishing among groups of organisms (Middelburg, 2014). As PLFA degrade rapidly after cell death, they therefore largely reflect the activity of living cells (Boschker and Middelburg, 2002). The combination of ^{13}C stable isotope labelling with biomarkers analyses and particulate organic carbon has been used to determine production rates at taxon-specific (Dijkman et al., 2009) and community level (Van den Meersche et al., 2004, 2011; De Kluijver et al., 2010, 2013).

To date, two experiments have focused on the effect of ocean acidification on the flow of carbon within plankton communities through the use of ^{13}C stable isotope labelling combined with biomarkers analyses. The first experiment was performed in the frame of the PeECE III project (Riebesell et al., 2008) in land-based mesocosms following initial nutrient additions (N and P). Group specific primary production rates increased with elevated pCO_2 during the post-bloom period, while no effects were found on phytoplankton-bacteria coupling nor on export rates (De Kluijver et al., 2010). The second experiment was performed in Arctic waters using large offshore mesocosms (Riebesell et al., 2013). Heterotrophic bacteria and two phytoplankton groups were distinguished based on their PLFA composition: mixotroph and autotrophic phytoplankton (De Kluijver et al., 2013). While no effects of CO_2 on particulate organic carbon (POC) production rates were detected before nutrient addition, POC production rates decreased with increasing partial pressure of CO_2 (pCO_2) after nutrient addition. In contrast, no CO_2 effects on bacterial production were highlighted both under nutrient-depleted or -replete conditions. Depending on the experimental period considered, positive or negative effects of CO_2 on phytoplankton and mixotroph production rates, zooplankton grazing and export of detritus were highlighted. The effects of ocean acidification during this experiment were subtle and different for each phase (before and after nutrient addition).

Most of the experiments conducted at community level (including mesocosm experiments) have been performed during a natural or artificial phytoplankton bloom that only occurs during a restricted period of the year and may not reflect the physiological state of plankton community and ecosystem trophic state for most of the year. There is therefore a strong lack of data for warm, low nutrient and productivity regions although these areas represent a vast majority of the surface ocean (>60%, Longhurst et al., 1995). However, a recent study in the Northwestern Mediterranean sea has shown a substantial effect of ocean acidification on plankton communities (phytoplankton abundances and bacterial activities and abundances) under very low nutrient concentrations (Sala et al., 2015) in 200 L laboratory mesocosms (controlled temperature, light intensity and light–dark cycles).

The Mediterranean Sea is oligotrophic for most of the year although several biogeographical provinces have been identified (D'Ortenzio and D'Alcalà, 2009). The pH decrease in this region has been estimated to be ~0.15 pH units since the industrial revolution (Touratier and Goyet, 2009) and an additional decrease of 0.3–0.4 units is foreseen for the end of the century (Geri et al., 2014). The effect of ocean acidification on plankton communities has been investigated based on mesocosm experiments conducted in two different sites of the Northwestern Mediterranean Sea (Gazeau et al., 2017a). This manuscript reports on the first ^{13}C labelling study on Mediterranean plankton communities in the frame of a mesocosm experiment focused on ocean acidification.

2. Material and methods

2.1. Study sites, experimental set-up and sampling

Two mesocosm experiments were carried out: one in the Bay of Calvi (BC; Corsica, France) in June–July 2012 and the other in the Bay of Villefranche (BV; France) in February–March 2013. The experimental set-up and mesocosm characteristics are described in Gazeau et al. (2017a). In brief, for each experiment, nine mesocosms of ca. 50 m^3 (2.5 m in diameter and 12 m maximum depth) were deployed for 20 and 11 days in BC and BV, respectively. Once the bottom of the mesocosms was closed, acidification of the mesocosms was performed over 4 days by homogenous addition of various volumes of CO_2-saturated seawater to obtain a pCO_2 gradient from ambient levels to an intended 1250 µatm, with three control mesocosms (C1, C2 and C3) and six mesocosms with increasing pCO_2 (P1 to P6). In BC, the six targeted elevated pCO_2 levels were P1: 550, P2: 650, P3: 750, P4: 850, P5: 1000 and P6: 1250 µatm. In BV, the levels were P1: 450, P2: 550, P3: 750, P4: 850, P5: 1000 and P6: 1250 µatm. Mesocosms were grouped in clusters of 3 with each cluster containing a control, a medium and a high pCO_2 level (cluster 1: C1, P1, P4; cluster 2: C2, P2, P5 and cluster 3: C3, P3, P6). During the last day of CO_2 saturated seawater addition, ^{13}C sodium bicarbonate ($NaH^{13}CO_3$; 99%) was added to each mesocosm to increase the isotopic level ($\delta^{13}C$ signature) of the dissolved inorganic carbon pool ($\delta^{13}C$-DIC) to ca. 200‰ in BC and 100‰ in BV. In BC, on day 11, a second addition of $NaH^{13}CO_3$ was performed to better constrain production rates and this resulted in a further enrichment of the DIC pool to ca. 270‰.

Every morning, depth-integrated samplings (0–10 m) were performed using 5 L Hydro-Bios integrated water samplers and sampled seawater was used for various analyses such as dissolved inorganic carbon and total alkalinity that were used to compute integrated pH and pCO_2 levels (Gazeau et al., 2017a), particulate organic matter measured on an elemental analyzer (Gazeau et al., 2017a), nitrate + nitrite (NO_x) and phosphate (PO_4^{3-}) measured at nanomolar level by Liquid Waveguide Capillary Cell (Louis et al., 2017), ammonium concentrations measured using an autoanalyser (Skalar) in BC and using a manual fluorometric method in BV (see Gazeau et al., 2017a, for more details), microbial abundances by flow cytometry (Celussi et al., 2017) and pigment concentrations measured by high performance liquid chromatography (Gazeau et al., 2017b). Daily samples for δ^{13}C-DIC, δ^{13}C-particulate organic carbon (δ^{13}C-POC) and δ^{13}C-phospholipid derived fatty acids (δ^{13}C-PLFA) were taken at the beginning (day 0–15 in BC and day 0–4 in BV) and every second day toward the end of the experiments. The sediment traps were emptied every day in BC or every other day in BV and samples were immediately preserved with pH buffered formaldehyde. In BC, a single zooplankton net haul (200 μm mesh size) was performed in each mesocosm at the end of the experiment so as not disturb the mesocosms during the experiment. Unfortunately, in BV, a storm caused an unintended opening of the mesocosms on day 13 (Gazeau et al. 2017a, for details) and no zooplankton net haul could be done during this experiment.

For δ^{13}C-DIC analyses, 20 mL of sampled seawater was gently transferred to glass vials avoiding bubbles and vials were sealed after being poisoned with 10 μL saturated $HgCl_2$ and stored upside-down at room temperature in the dark pending analysis. For δ^{13}C-POC, sampled seawater (0.5–1 L) was immediately filtered on pre-weighed and pre-combusted 25 mm GF/F. Filters were dried at 60 °C and stored in a dry place pending analysis. Samples for δ^{13}C-PLFA analyses (~4 L) were filtered through 47 mm pre-combusted GF/F filters, which were subsequently stored at −80 °C. Zooplankton samples of the final net haul were transferred to 0.2 μm filtered seawater for 30 min to empty their guts. One to ten individuals of the two species *Paracalanus* spp. and *Oncaea* spp., that were found in nearly all mesocosms, were transferred to pre-combusted tin cups and were stored at −80 °C for organic δ^{13}C analyses. For sediment trap samples, swimmers larger than 1 mm were removed (and discarded) and the remaining material was rinsed, centrifuged and freeze-dried. In BC, as a consequence of low amounts of material especially at the end of the experiment, daily sediment traps samples were pooled as follows: days 5–7, 8–10, 11–14 and 15–19. Total particulate matter was weighed for flux determination and subsamples were used for POC and δ^{13}C-POC measurements.

2.2. Laboratory analyses

Sample preparations and measurements for δ^{13}C analyses were performed at the Netherlands Institute of Sea Research (NIOZ-Yerseke; The Netherlands) except for measurements of sediment traps δ^{13}C-POC in BV that were performed at the Laboratoire d'Océanographie de Villefranche (LOV; France). At NIOZ-Yerseke, δ^{13}C-POC samples were analyzed on an elemental analyzer (EA; Thermo Electron Flash 1112) coupled to a Delta V isotope ratio mass spectrometer (IRMS). At LOV, δ^{13}C-POC samples were analyzed on an elemental analyzer (Elementar Vario Pyrocube) coupled to an Isoprime 100 IRMS. For δ^{13}C-DIC analyses, a helium headspace (3 mL) was created in the vials and samples were acidified with 2 μL of phosphoric acid (H_3PO_4, 99%) to transfer all DIC to gaseous CO_2. After equilibration, the CO_2 concentration in the headspace and its isotopic composition were measured on an EA-IRMS. PLFA were extracted using a modified Bligh & Dyer method (Middelburg et al., 2000). In brief, after extraction of total lipids in a methanol:-chloroform mix, lipids were separated into different polarity classes on a column separation using previously heat activated silica. After elution with chloroform and acetone, the methanol fraction was collected and PLFA were derivatized to fatty acid methyl esters (FAME). The standards 12:0 and 19:0 were used as internal standards. Concentrations and δ^{13}C of individual PLFA were measured using gas chromatography-combustion isotope ratio mass spectrometry (GC-c-IRMS). In BC, due to very low concentrations, daily PLFA samples were pooled by two days after the extraction step.

2.3. Data analyses

Carbon isotope data are expressed in the delta notation (δ) relative to Vienna Pee Dee Belemnite (VPDB) standard and are presented as specific enrichment ($\Delta\delta^{13}$C) and ^{13}C incorporation (Middelburg, 2014). The specific enrichment $\Delta\delta^{13}$C was calculated as $\delta^{13}C_{sample} - \delta^{13}C_{background}$ with $\delta^{13}C_{background}$ being the isotope ratio under natural conditions (before ^{13}C addition). The carbon isotope ratio was calculated as $R_{sample} = (\delta^{13}C_{sample}/1000 + 1) \times R_{VPDB}$, with $R_{VPDB} = 0.011237$. The ^{13}C fraction was calculated as: $^{13}F = {}^{13}C/({}^{13}C + {}^{12}C) = R/(R + 1)$. The excess ^{13}C was obtained as $\Delta^{13}F = {}^{13}F_{sample} - {}^{13}F_{background}$. Incorporation was then calculated as ^{13}C-incorporation $= \Delta^{13}F \times C$ (μmol ^{13}C L^{-1}; De Kluijver et al., 2010) with C being POC or PLFA concentrations in μmol C L^{-1}. In order to directly compare values between mesocosms, data were corrected for the different initial δ^{13}C-DIC using a correction factor calculated as the ratio between δ^{13}C-DIC in each mesocosm to the average δ^{13}C-DIC in all mesocosms at day 0. This ratio varied from 0.92 to 1.21 in BC and from 0.72 to 1.22 in BV. δ^{13}C-DIC data were corrected for air-sea gas exchanges using the method described in Czerny et al. (2013).

Different PLFA were detected depending on the experiment and higher PLFA concentrations and more diversity were measured in BV than in BC. Only a few PLFA are taxon specific with many PLFA shared by several groups (Dalsgaard et al., 2003) and in the same taxon there are strain specific differences in PLFA composition (Dijkman and Kromkamp, 2006). Therefore, an approach combining several indicators is recommended to infer the plankton composition (Dalsgaard et al., 2003). Two specific PLFA, detected in both experiments (ai15:0 and i15:0), were used to identify heterotrophic bacteria (Kaneda, 1991). For phytoplankton, identification at the species or taxon level was too complex, and only two phytoplankton groups were distinguished by combining information on PLFA ratios and PLFA biomarker attribution based on the literature. In a first step, for both experiments, the ratios 16:1ω7/16:0 < 1 as well as 20:5ω3/22:6ω3 <1 indicated a low living biomass and the presence of aggregates from senescent and/or degrading diatoms as well as dominance of dinoflagellates and flagellates over diatoms (Tolosa et al., 2004; Balzano et al., 2011). These ratios allow inferring that C16 and 20:5ω3 are not specifically attributed to diatoms but to other phytoplankton groups sharing the same PLFA. In BC, PLFA that showed a delayed δ^{13}C incorporation (18:1ω9c, 20:5ω3 and 22:6ω3) likely representing heterotrophic dinoflagellates and flagellates as well as some haptophytes (Dalsgaard et al., 2003; Brinis et al., 2004; Dijkman and Kromkamp, 2006; Rossi et al., 2006), were grouped. Their weighted δ^{13}C ratio and sum of concentrations were used to describe a general slow-growing phytoplankton group termed Phyto2. The PLFA that showed a comparatively fast incorporation were 16:2ω4, 18:4ω3 and 18:3ω3 and their weighted δ^{13}C ratio was used to characterize fast-growing phytoplankton (Phyto1) comprising cyanophytes, chlorophytes (prasinophyceae and chlorophyceae) and other haptophytes (Viso and Marty, 1993; Dalsgaard et al., 2003; Dijkman and Kromkamp, 2006). In BV, a slow-growing phytoplankton group

Phyto2 containing 16:4ω3, 20:5ω3 and 22:6ω3 was considered and comprised heterotrophic dinoflagellates, some haptophytes and some diatoms. The fast incorporating group Phyto1 contained the following PLFA: 16:2ω4, 18:2ω6c, 18:3ω3, 18:4ω3, 18:5ω3(12−15) and 18:5ω3(12−16), and comprised cryptophytes, some haptophytes, chlorophytes and autotrophic dinoflagellates (Viso and Marty, 1993; Dalsgaard et al., 2003; Dijkman and Kromkamp, 2006; Adolf et al., 2007; Taipale et al., 2013, 2009). The sum of characteristic PLFA concentrations were converted to total carbon concentrations using conversion factors of 0.01, 0.06 and 0.05 μg C PLFA/μg C for heterotrophic bacteria, fast-growing Phyto1 and slow-growing Phyto2, respectively (Van Den Meersche et al., 2004; Dijkman et al., 2009; De Kluijver et al., 2013).

Primary production rates were calculated based on ^{13}C incorporation in POC as well as in PLFA characteristic of each phytoplankton group and for each time interval using the equation:

$$PP = \left[\Delta(^{13}F_{biomass} \cdot C_{biomass})/\Delta t - {}^{13}F_{mean;biomass}(\Delta C_{biomass}/\Delta t)\right] \times / \left[{}^{13}F_{mean;DIC} - {}^{13}F_{mean;biomass}\right] \quad (1)$$

in μmol C L^{-1} d^{-1} with, $^{13}F_{biomass}$ the ^{13}C fraction in the considered biomass (PLFA fast- and slow-growing phytoplankton or POC), $C_{biomass}$ the concentration of the considered biomass in μmol C L^{-1}, Δt is the time interval in days, $^{13}F_{mean;biomass}$ is the average ^{13}C fraction in the considered biomass (PLFA or POC) for the time interval and $^{13}F_{mean;DIC}$ is the average ^{13}C fraction in DIC for the considered time intervals.

By the end of the experiment, stable isotope patterns approached steady state and the ratio of the enrichment in consumers ($\Delta\delta^{13}C_{cons}$) to the enrichment of the substrate ($\Delta\delta^{13}C_{subst}$) can then be used to quantify the dependency of consumers on the resource (Van Oevelen et al., 2006; Middelburg, 2014).

2.4. Model description

Having isotope enrichment data ($\Delta\delta^{13}C$) at multiple time steps allows using a simple sink-source isotope ratio model based on that of Hamilton et al. (2004) in which the isotopic composition of a consumer is altered by the uptake of the source compartments minus any losses. This model is based on two assumptions: that labelled DIC concentration is known within the mesocosm at each time point and that the biomass of consumers is at steady state with time. This model allows estimating the turnover rate of phytoplankton and heterotrophic bacterial groups (r, d^{-1}). Here we apply a phytoplankton-bacteria-detritus model, with two phytoplankton types (Phyto1 and Phyto2 for the fast and slow incorporation groups, respectively), to model the ^{13}C data of this study:

$$d\Delta\delta^{13}C_{Phyto1}/dt = r_{Phyto1}\left(\Delta\delta^{13}C_{DIC} - \Delta\delta^{13}C_{Phyto1}\right) \quad (2)$$

$$d\Delta\delta^{13}C_{Phyto2}/dt = r_{Phyto2}\left(\Delta\delta^{13}C_{DIC} - \Delta\delta^{13}C_{Phyto2}\right) \quad (3)$$

$$d\Delta\delta^{13}C_{bact}/dt = r_{bact}\left(\Delta\delta^{13}C_{Phyto1} - \Delta\delta^{13}C_{bact}\right) \quad (4)$$

$$d\Delta\delta^{13}C_{det}/dt = r_{Phyto1}\left(\Delta\delta^{13}C_{Phyto1} - \Delta\delta^{13}C_{det}\right) + r_{Phyto2}\left(\Delta\delta^{13}C_{Phyto2} - \Delta\delta^{13}C_{det}\right) + r_{bact}\left(\Delta\delta^{13}C_{bact} - \Delta\delta^{13}C_{det}\right) \quad (5)$$

This model was implemented in the R software (R core team 2013), using the R-packages packages deSolve (Soetaert et al., 2010) and fitted to the data using the R-package FME (Soetaert and Petzoldt, 2010). It was applied to the experimental periods of 20 and 9 days in BC and BV, respectively. More details and earlier applications of the model can be obtained in Van Oevelen et al. (2006) and De Kluijver et al. (2010). This simple modelling approach allows derivation of model parameters with uncertainty.

2.5. Statistics

In order to identify differences between pCO_2 treatments, stepwise multiple linear regression analyses were performed to establish relationships between estimated parameters and processes and environmental/experimental conditions including pCO_2. Other environmental conditions that have been considered were temperature, salinity and nutrients (NO_x, NH_4^+ and PO_4^{3-}). Integrated levels of temperature and salinity were acquired through daily CTD casts performed in each mesocosm. Furthermore, cumulative productions were calculated as the sum of production rates calculated from Equation (1) for the available experimental period and were related to increased pCO_2 levels (averages during the experiments) using linear regression. All regressions were performed using the R software (version 3.1; www.r-project.org) and were considered significant at a probability $p < 0.01$ and marginally significant at a probability $p < 0.05$.

3. Results

3.1. Environmental and experimental conditions during both experiments

Ambient pCO_2 levels were higher in BC in summer as compared to BV in winter (~450 *vs.* 350 μatm respectively; Fig. S1). While pCO_2 levels slightly decreased in BC after the acidification phase during the course of the experiment, especially for high CO_2 mesocosms (P5 and P6), drops in pCO_2 levels were much more important in BV due to strong winds (see Gazeau et al. 2017a for more details) with mesocosms P1 to P4 showing very similar levels by the end of the experiment. In BC, NO_x and PO_4^{3-} were very low: NO_x always remained below 150 nmol L^{-1} while PO_4^{3-} average was 9 ± 4 nmol L^{-1} (data not shown; Louis et al., 2017). Ammonium levels averaged 0.37 ± 0.18 μmol L^{-1} (data not shown) without specific time evolution. This N/P co-limitation likely prevented the development of a phytoplankton bloom as shown by a mean chlorophyll *a* concentration of 70 ± 10 ng L^{-1} (Fig. S1). Haptophytes and cyanophytes were dominating the phytoplankton community (data not shown; Gazeau et al., 2017b).

In BV, nutrient levels were initially higher than in BC but NO_x and PO_4^{3-} were rapidly consumed during the acidification period leading to an unusual, at this period of the year, N and P co-limitation when the experiment started (data not shown; Louis et al., 2017). Ammonium concentrations were lower than in BC averaged 0.05 ± 0.01 μmol L^{-1} (data not shown) and tended to decrease during the experiment. The average chlorophyll *a* concentration was however much higher (987 ± 147 ng L^{-1}) than in BC (Fig. S1) and the community was dominated by cryptophytes and haptophytes (data not shown; Gazeau et al., 2017b).

Chlorophyll *a* was not affected by CO_2 during both experiments (Gazeau et al., 2017b) and displayed a stationary trend over time in BC while slightly decreasing during the experiment in BV (Fig. S1). Nutrient concentrations were also not impacted by CO_2 during both experiments (Louis et al., 2017). Heterotrophic bacteria abundances did not respond to increase pCO_2 (Celussi et al., 2017).

3.2. Carbon flow in the Bay of Calvi

3.2.1. Labelling results: DIC and POC

The addition of $NaH^{13}CO_3$ led to an increase of $\Delta\delta^{13}$C-DIC in all mesocosms to an average (±SD) of 224 ± 16‰ that steadily decreased to a minimum of 194 ± 12‰ at day 10 before the second addition was performed. This latter further increased $\Delta\delta^{13}$C-DIC to 270 ± 13‰ (Fig. 1a). The ^{13}C-DIC concentration varied during the whole experimental period from 7.3 to 4.2 µmol ^{13}C L^{-1}, accounted for 0.19–0.30% of total DIC concentration and followed the same temporal pattern as described for $\Delta\delta^{13}$C-DIC. The decrease in ^{13}C-DIC concentrations occurred in all mesocosms independent of pCO_2 level. Losses through air-sea exchange were negligible (<0.7% ^{13}C-DIC; data not shown).

Incorporation into POC was rapid and a first plateau starting at day 9 was reached with an average (±SD) $\Delta\delta^{13}$C-POC in all mesocosms of 86 ± 8‰. The second addition of $NaH^{13}CO_3$ on day 11 led to a further increase in $\Delta\delta^{13}$C-POC until day 15 when a second plateau was reached (average ± SD of all mesocosms: 122 ± 18‰; Fig. 1a). The ^{13}C-POC concentration varied, following the same temporal pattern as for $\Delta\delta^{13}$C-POC, from 3.6 to 58.2 10^{-4} µmol ^{13}C L^{-1}. The ratio of $\Delta\delta^{13}$C-POC/$\Delta\delta^{13}$C-DIC reached a maximum of 0.54 ± 0.04 (average ± SD of all mesocosms) at the end of the experiment and differences among mesocosms were not related to pCO_2 levels (Table 1). Ratios remained below 1 indicating a large inert (non-reacting) detritus pool.

3.2.2. Phytoplankton and bacteria dynamics: labelling and biomass

The averaged $\Delta\delta^{13}$C-Phyto2 steadily increased to an average between all mesocosms (±SD) of 123 ± 16‰ and the second $NaH^{13}CO_3$ addition on day 11 allowed an additional increase to 167 ± 27‰ (Fig. 1a). The fast-growing phytoplankton (Phyto1) incorporated ^{13}C much faster and on day 6 a first saturation plateau was reached at an average (±SD) between all mesocosms of 170 ± 12‰. After the second $NaH^{13}CO_3$ addition, $\Delta\delta^{13}$C-Phyto1 increased again until the end of the experiment to 187 ± 27‰ (average of all mesocosms ± SD; Fig. 1a). The $\Delta\delta^{13}$C-bacteria steadily increased to reach a final average (±SD) maximum of 136 ± 17‰ (Fig. 1a).

The final ratios of $\Delta\delta^{13}$C-Phyto1/$\Delta\delta^{13}$C-DIC and $\Delta\delta^{13}$C-Phyto2/$\Delta\delta^{13}$C-DIC reached an averaged (±SD) maximum of 0.82 ± 0.07 and 0.73 ± 0.06, respectively. The ratio $\Delta\delta^{13}$C-bacteria/$\Delta\delta^{13}$C-all phytoplankton averaged 0.80 ± 0.15 at the end of the experiment and were independent of pCO_2 levels (Table 1). Heterotrophic bacteria growth was based on Phyto1 or Phyto2 products as bacteria isotope ratios ($\Delta\delta^{13}$C) were below isotope ratios of fast and slow growing phytoplankton. The ^{13}C content of Phyto1, Phyto2 and heterotrophic bacteria, used to estimate production rates, increased during the experiment (Fig. 2a–c) until day 15 after which labelling reached a plateau.

Biomass of Phyto1 was very low and increased from an average (±SD) between all mesocosms of 0.013 ± 0.003 to 0.03 ± 0.01 µmol C L^{-1} (Fig. 3a), reflecting the increase in chlorophyll *a* until day 12 (Fig. S1). The estimated biomass of Phyto2 tended to increase over the experimental period from an average (±SD) between all mesocosms of 0.06 ± 0.01 to 0.12 ± 0.04 µmol C L^{-1} (Fig. 3a). Heterotrophic bacterial biomass based on PLFA varied from an average (±SD) between all mesocosms of 0.021 ± 0.007 to 0.06 ± 0.03 µmol C L^{-1} (Fig. 3a) and tended to increase during the experiment although this was not evidenced based on flow cytometry data (Celussi et al., 2017; see Fig. S1). No relationships between pCO_2 and biomasses of the different compartments were found using the stepwise multiple regression analysis approach (Table 2) but with nutrient concentrations and temperature.

3.2.3. Primary production based on POC and PLFA

Based on POC labelling, net community production rates (NCP-^{13}C) globally averaged 0.15 ± 0.01 µmol C L^{-1} d^{-1} with large variations between mesocosms and sampling days. Stepwise analyses reveal no effect of increasing pCO_2 and no significant relationships with any other environmental parameters (Table 2). Meanwhile, cumulative productions ranged from 1.12 to 2.29 µmol C L^{-1} with no significant trend with increasing pCO_2 (Fig. 4a; n = 9, r = − 0.51, $p > 0.05$). Both phytoplankton groups did not show any particular temporal trend and the Phyto2 group was more productive with the lowest cumulative production in P6 (0.02 µmol C L^{-1}) and the highest in P2 (0.19 µmol C L^{-1}). No linear trend with increasing pCO_2 levels was observed for both phytoplankton groups on cumulative productions (Fig. 4b; n = 9, r = −0.49, $p > 0.05$ and n = 9, r = −0.35, $p > 0.05$, for Phyto1 and Phyto2, respectively). Stepwise analyses reveal no effect of increasing pCO_2 and no significant relationships with any other environmental parameter for the primary production of Phyto2 (Table 2) while Phyto1 production rates followed the same trend than temperature (Table 2).

3.2.4. Zooplankton and sediment traps

Specimens of the copepod *Paracalanus* spp. were present in samples from all mesocosms except P1 and P2 and specimens of *Oncaea* spp. were found in all samples except for mesocosm P3. *Paracalanus* showed a higher specific enrichment ($\Delta\delta^{13}$C; average 108 ± 10‰; Fig. 5) than *Oncaea* (average 60 ± 10‰). Both species were less labelled in P6 but there was no significant effect of pCO_2

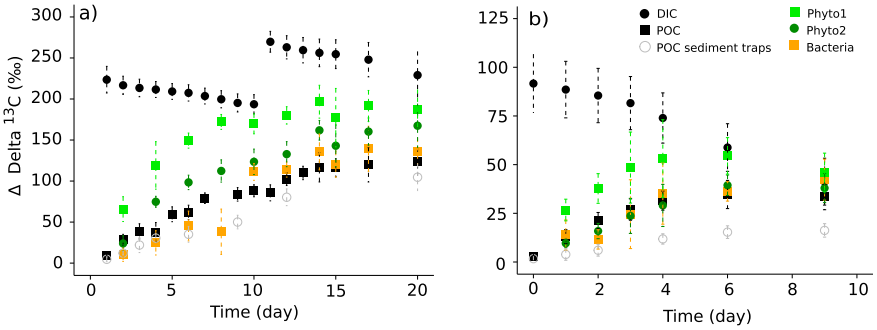

Fig. 1. Average $\Delta\delta^{13}$C (±SD) in the nine mesocosms deployed in a) the Bay of Calvi in summer 2012 and b) the Bay of Villefranche in winter 2013, for dissolved inorganic carbon (DIC; black points), particulate organic carbon in the water column (POC; black squares), fast-growing phytoplankton (Phyto1; light green squares), slow-growing phytoplankton (Phyto2; dark green points) and heterotrophic bacteria (orange squares). (For interpretation of the references to colour in this figure legend, the reader is referred to the web version of this article.)

Table 1
Final ratio of $\Delta\delta^{13}C$ enrichment and results of linear regression in the different particulate organic compartments in the Bay of Calvi (at day 20) and Villefranche (at day 9, except for heterotrophic bacteria: at day 6). Bulk particulate organic carbon (POC), fast- and slow-growing phytoplankton groups (Phyto1 and 2, respectively) and heterotrophic bacteria (bact), relative to final ^{13}C enrichment of dissolved inorganic carbon (DIC) or all phytoplankton (Phyto1 + Phyto2). ND: not determined.

	C1	C2	C3	P1	P2	P3	P4	P5	P6	r, *p-value*
Bay of Calvi										
$\Delta\delta^{13}C$-POC/$\Delta\delta^{13}C$-DIC	0.48	0.54	0.49	0.55	0.56	0.58	0.55	0.61	0.51	0.36, *0.16*
$\Delta\delta^{13}C$-Phyto1/$\Delta\delta^{13}C$-DIC	0.90	0.77	0.82	0.85	0.88	0.75	0.70	0.89	0.81	−0.15, *0.35*
$\Delta\delta^{13}C$-Phyto2/$\Delta\delta^{13}C$-DIC	0.77	0.60	0.75	0.74	0.80	0.72	0.72	0.75	0.71	0.05, *0.45*
$\Delta\delta^{13}C$-bact/$\Delta\delta^{13}C$-all phytoplankton	1.07	0.70	0.95	0.63	0.80	0.66	0.72	ND	0.84	−0.21, *0.31*
Bay of Villefranche										
$\Delta\delta^{13}C$-POC/$\Delta\delta^{13}C$-DIC	0.68	0.94	0.77	0.73	0.93	0.84	1.04	0.82	0.78	−0.01, *0.49*
$\Delta\delta^{13}C$-Phyto1/$\Delta\delta^{13}C$-DIC	1.11	1.26	1.06	1.03	1.27	1.13	1.31	1.09	0.98	−0.40, *0.14*
$\Delta\delta^{13}C$-Phyto2/$\Delta\delta^{13}C$-DIC	0.95	1.08	0.87	0.79	1.10	0.92	1.12	0.92	0.77	−0.39, *0.15*
$\Delta\delta^{13}C$-bact/$\Delta\delta^{13}C$-all phytoplankton	0.65	0.71	0.70	0.89	ND	0.89	ND	0.75	0.83	0.45, *0.16*

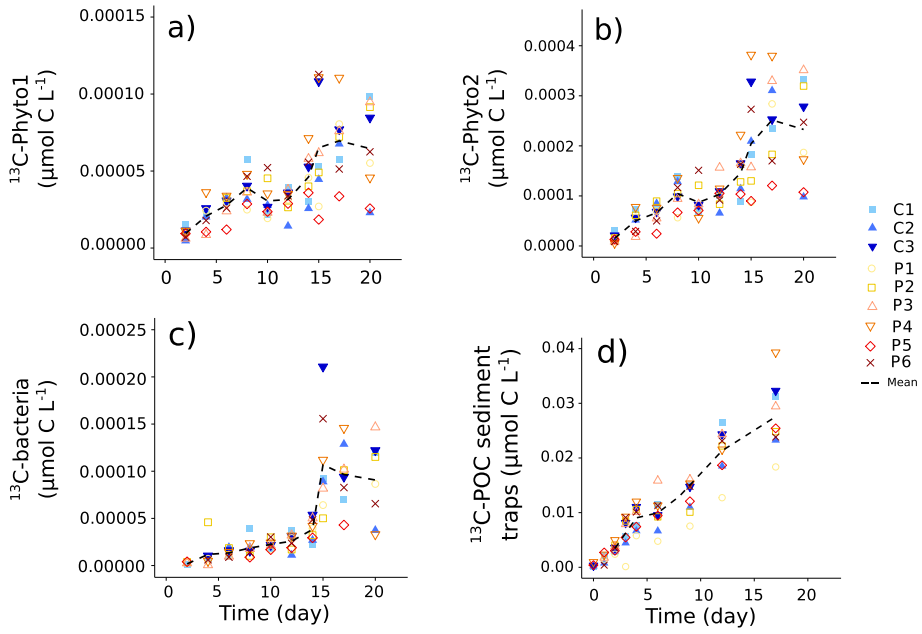

Fig. 2. ^{13}C-biomass (µmol ^{13}C L^{-1}) in the nine mesocosms (C1 to P6) deployed in the Bay of Calvi in summer 2012 for a) fast-growing phytoplankton (Phyto1), b) slow-growing phytoplankton (Phyto2), c) heterotrophic bacteria and d) settling particles.

on zooplankton ^{13}C enrichment (Fig. 5; *Paracalanus*: n = 7, r = −0.73, $p > 0.05$; *Oncaea*: n = 8, r = −0.31, $p > 0.05$).

Transfer of ^{13}C to sediment traps was fast, as after 2 days an increase in sediment-trap ^{13}C-POC was measured and ^{13}C-POC of settlings particles increased with time (Fig. 2d). The stepwise multiple regression analysis revealed no relationship between pCO_2 and labelled settling particles but a significant relationship with temperature, as both parameters increased during the experimental period, and a marginal relationship with NO_x (Table 2). Cumulative ^{13}C labelling in settling particles was also independent of pCO_2 (linear regression on daily cumulative labelled materials: n = 9, r = 0.23, $p > 0.05$).

3.3. Carbon flow in the Bay of Villefranche

3.3.1. Labelling results: DIC and POC

The addition of $NaH^{13}CO_3$ led to an increase in $\Delta\delta^{13}C$-DIC to 92 ± 15‰ (average ± SD between all mesocosms) that steadily decreased to a minimum of 41 ± 12‰ until day 9 (Fig. 1b). The ^{13}C-DIC concentration varied during the whole experimental period between an average between all mesocosms of 0.6 and 2.9 µmol ^{13}C L^{-1} and followed the same pattern as described for $\Delta\delta^{13}C$-DIC. Losses by air-sea exchange calculated during the experiment were more important than in BC and were dependent on the considered mesocosm. Control mesocosms presented similar negative air-sea fluxes while perturbed mesocosms (P1 to P6) presented positive fluxes with a ^{13}C outgassing up to 3% of ^{13}C-DIC in the most acidified mesocosms (P5 and P6; data not shown), explaining partly the decrease in ^{13}C-DIC observed during the experiment.

Incorporation into POC was rapid and on day 6 a plateau was reached with $\Delta\delta^{13}C$-POC (average ± SD of 35 ± 7‰; Fig. 1b) and with a final value on day 9 of 33 ± 7‰. ^{13}C-POC concentrations varied, following the same pattern as for $\Delta\delta^{13}C$-POC, from 1.3 to $48.8 \cdot 10^{-4}$ µmol ^{13}C L^{-1}. The ratio of $\Delta\delta^{13}C$-POC/$\Delta\delta^{13}C$-DIC reached a average (±SD) maximum of 0.83 ± 0.11 at the end of the experiment when nearly all the particulate material had been labelled and was independent of pCO_2 levels (Table 1).

3.3.2. Phytoplankton and bacteria dynamics: biomass and labelling

The $\Delta\delta^{13}C$-Phyto2 steadily increased until day 9—38 ± 7‰ while $\Delta\delta^{13}C$-Phyto1 reached 46 ± 10‰. The $\Delta\delta^{13}C$ of heterotrophic bacteria was similar to $\Delta\delta^{13}C$-Phyto2 with an average between all mesocosms (±SD) of 36 ± 5‰ on day 6 (Fig. 1b) and to 42 ± 11‰ on day 9, however only values for C1 and C3 are available for the last

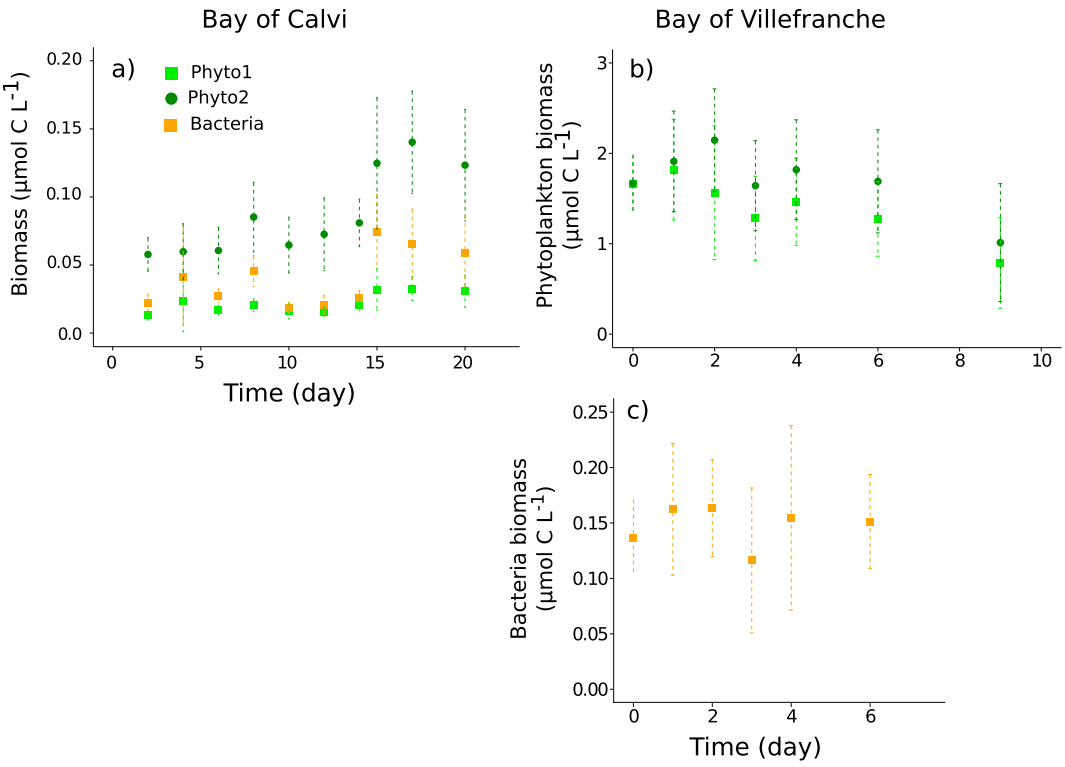

Fig. 3. Average biomass concentration in all nine mesocosms deployed in the a) Bay of Calvi (summer 2012) and b) and c) in the Bay of Villefranche (winter 2013) based on phospholipids derived fatty acids (PLFA) concentrations for fast- and slow-growing phytoplankton (Phyto1 and 2, respectively) and heterotrophic bacteria.

Table 2
Stepwise multiple regression analysis between estimated parameters/processes and environmental parameters during both experiments. Estimated parameters/processes were biomasses of fast and slow-growing phytoplankton (Phyto1 and 2, respectively) and heterotrophic bacteria, ^{13}C content of settlings particles (^{13}C-sed) and production rates based on particulate organic carbon labelling (NCP-^{13}C) as well as group-specific (fast-growing phytoplankton: PP-Phyto1 and slow-growing phytoplankton: PP-Phyto2) production rates using phospholipids derived fatty acids (PLFA) biomarkers. Environmental variables: salinity (S), temperature (T), dissolved inorganic nitrogen and phosphorus (nitrate + nitrite: NO_x, ammonium: NH_4^+ and phosphate: PO_4^{3-}), and partial pressure of CO_2 (pCO_2) ($p < 0.05^*$; $p < 0.01^{**}$; NS non significant).

	Bay of Calvi							Bay of Villefranche						
	F	Adj r^2	dF	Overall p-value	Variables	Sign	p-value	F	Adj r^2	dF	Overall p-value	Variables	Sign	p-value
Phyto1	21.19	0.29	96	<0.001	T^{**}	+	<0.001	3.47	0.17	23	0.048	NH_4^{+*}	+	0.033
					NO_x^{**}	+	0.004							
Phyto2	48.4	0.49	96	<0.001	T^{**}	+	<0.001	NS						
					NO_x^{**}	+	<0.001							
					NH_4^+	−	0.012							
Bacteria	16.1	0.25	88	<0.001	NO_x^{**}	+	0.004	NS						
					T^{**}	+	<0.001							
^{13}C-sed	228.2	0.85	77	<0.001	T^{**}	+	<0.001	29.22	0.81	27	<0.001	pCO_2^{**}	−	<0.001
					NO_x^*	+	0.034					NH_4^+	−	0.019
												PO_4^{3-*}	−	0.0021
												S^{**}	+	<0.001
NCP-^{13}C	12.02	0.13	141	<0.001	S	−	0.07	24.53	0.58	49	<0.001	NO_x^{**}	−	<0.001
					T	−	0.10					T^{**}	+	0.004
												S^{**}	−	<0.001
PP-Phyto1	7.15	0.12	85	0.00135	T^{**}	−	0.0003	40.29	0.80	35	<0.001	NO_x^{**}	−	<0.001
					PO_4^{3-*}	−	0.12					T^*	+	0.0017
												NH_4^+	+	0.0014
												S^{**}	−	<0.001
PP-Phyto2	4.4	0.10	85	0.0065	T^{**}	−	0.001	13.37	0.55	36	<0.001	NO_x^{**}	−	<0.001
					S^{**}	+	0.010					T^*	−	0.019
					PO_4^{3-}	−	0.041					S^{**}	−	<0.001

day. After that day, $\Delta\delta^{13}C$-DIC, POC and PLFA were at isotopic equilibrium and no other $NaH^{13}CO_3$ addition could be done to stimulate further ^{13}C incorporation into particulate matter (Fig. 1b) due to a storm event (see Material and methods).

Ratio of $\Delta\delta^{13}C$-Phyto1/$\Delta\delta^{13}C$-DIC and $\Delta\delta^{13}C$-Phyto2/$\Delta\delta^{13}C$-DIC reached an averaged (±SD) maximum of 1.1 ± 0.1 and 1.0 ± 0.1, respectively meaning that all ^{13}C was incorporated into particulate phytoplankton biomass (Table 1). Final ratio $\Delta\delta^{13}C$-bacteria/$\Delta\delta^{13}C$-all phytoplankton on day 6 averaged (±SD) 0.60 ± 0.07. All final ratios were independent of pCO_2 levels (Table 1).

The ^{13}C-biomasses showed more variability between mesocosms than during the experiment in BC (Fig. 6a–c) and

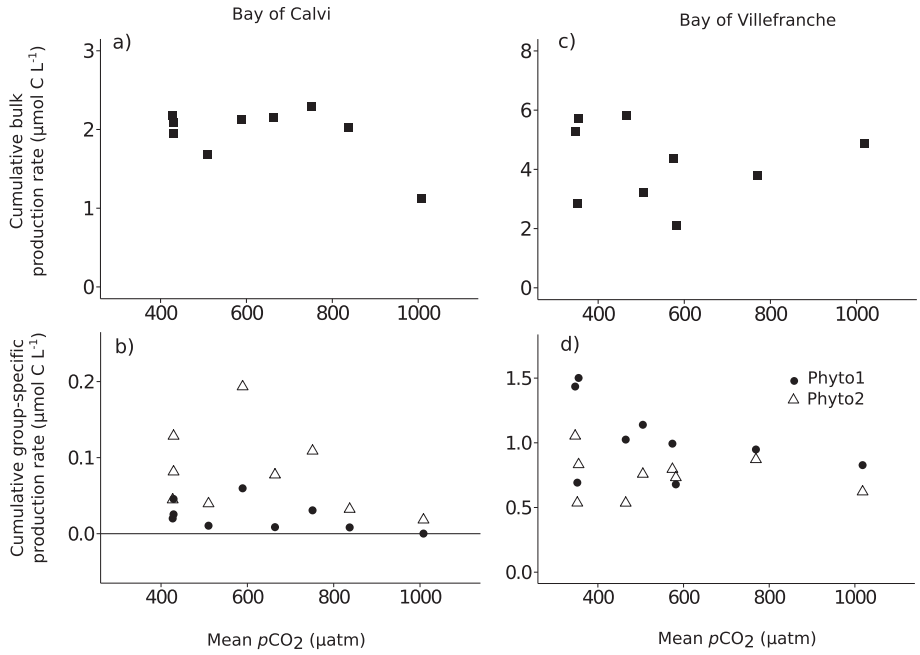

Fig. 4. Cumulative production based on bulk organic carbon (NCP-^{13}C; top) and phytoplankton group-specific production (bottom; full circles: fast-growing phytoplankton or Phyto1, empty triangles: slow-growing phytoplankton or Phyto2) as a function of mean partial pressure of CO_2 levels (mean pCO_2) in each mesocosm over the experimental period in the Bay of Calvi (left panels) and Villefranche (right panels).

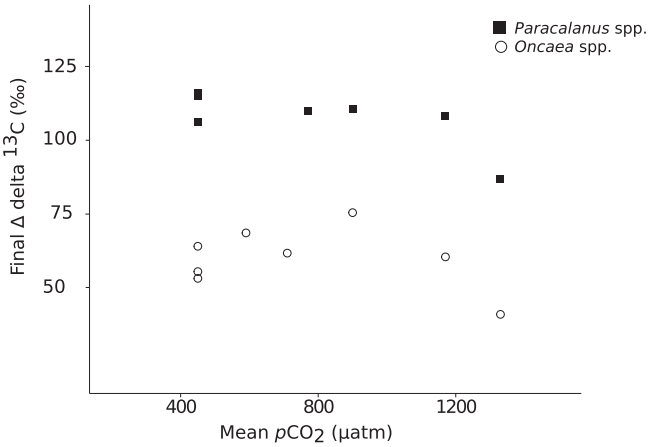

Fig. 5. Final isotopic signature ($\Delta\delta^{13}C$ in ‰) of the zooplankton species *Paracalanus* spp. and *Oncaea* spp. as a function of average partial pressure of CO_2 (pCO_2) levels in each mesocosm over the experimental period, during the experiment conducted in the Bay of Calvi in summer 2012.

heterotrophic bacteria were very difficult to identify based on PLFA especially at the end of the experiment. Fast- and slow-growing phytoplankton ^{13}C-biomasses increased during the experiment (Fig. 6a–c) until days 6 and decreased between day 6 and 9.

Biomasses estimated using PLFA for the two phytoplankton groups were higher than in BC (Fig. 3b) and biomasses tended to decrease over the course of the experiment (9 days) with a large variability between mesocosms as also observed with chlorophyll *a* concentrations (Fig. S1). During this experiment, fast- and slow-growing phytoplankton showed similar concentrations. Biomass of Phyto1 was on average (±SD) 1.7 ± 0.3 and 0.8 ± 0.5 µmol C L^{-1} on day −1 and 9 while biomass of Phyto2 was on average (±SD) 1.7 ± 0.3 and 1.0 ± 0.7 µmol C L^{-1} on day −1 and 9, respectively. Heterotrophic bacterial biomass based on PLFA was higher than in BC with an average (±SD) during the experiment 0.15 ± 0.02 µmol C L^{-1}, and showed no clear temporal trend (Fig. 3c) in contrast to flow cytometry data that showed an increase in heterotrophic bacteria cell abundances during the course of the experiment (Fig. S1). Stepwise multiple regression analyses did not reveal a pCO_2 effect on any of the estimated biomasses but a marginal relationship between Phyto1 and NH_4^+ (Table 2.).

3.3.3. Primary production based on POC and PLFA

Net community production based on the incorporation of ^{13}C into POC (NCP-^{13}C) decreased during the experiment from an average (±SD) between all mesocosms of 1.03 ± 0.24 to −0.09 ± 0.41 µmol C L^{-1} d^{-1}. As ^{13}C-POC was equilibrated already with ^{13}C-DIC on day 6, no estimate of NCP-^{13}C could be obtained for the rest of the experiment. Stepwise multiple regression analysis did not reveal any pCO_2 effect on this process (Table 2) but with salinity, temperature and NO_x. Cumulative productions from day 0–6 varied from 2.1 to 5.9 µmol C L^{-1} in P4 and P1 respectively and were not correlated to pCO_2 levels (Fig. 4c; n = 9, r = - 0.08, $p > 0.05$). In contrast to what has been observed in BC, the two considered phytoplankton groups presented a clear temporal trend based on their production rates. Production rates of slow-growing phytoplankton (Phyto2), were rather constant during the first four days of the experiment but further decreased with final cumulative productions ranging from 0.53 to 1.05 µmol C L^{-1} (Fig. 4d). Phyto1 presented higher cumulative production rates (Fig. 4d) although they decreased over the course of the experiment. Cumulative productions did not correlate with increasing pCO_2 levels (Fig. 4d; Phyto1: n = 9, r = −0.45, $p > 0.05$; Phyto2: n = 9, r = −0.17, $p > 0.05$). Stepwise multiple regression analysis did not reveal relationship with pCO_2 levels (Table 2) but as for NCP-^{13}C with salinity, temperature, NH_4^+ and NO_x.

3.3.4. Zooplankton and sediment traps

As mentioned in the Material and methods section, no samples were available for zooplankton. As in BC, transfer of ^{13}C to sediment traps was fast and on day 1 an increase in sediment-trap ^{13}C-POC

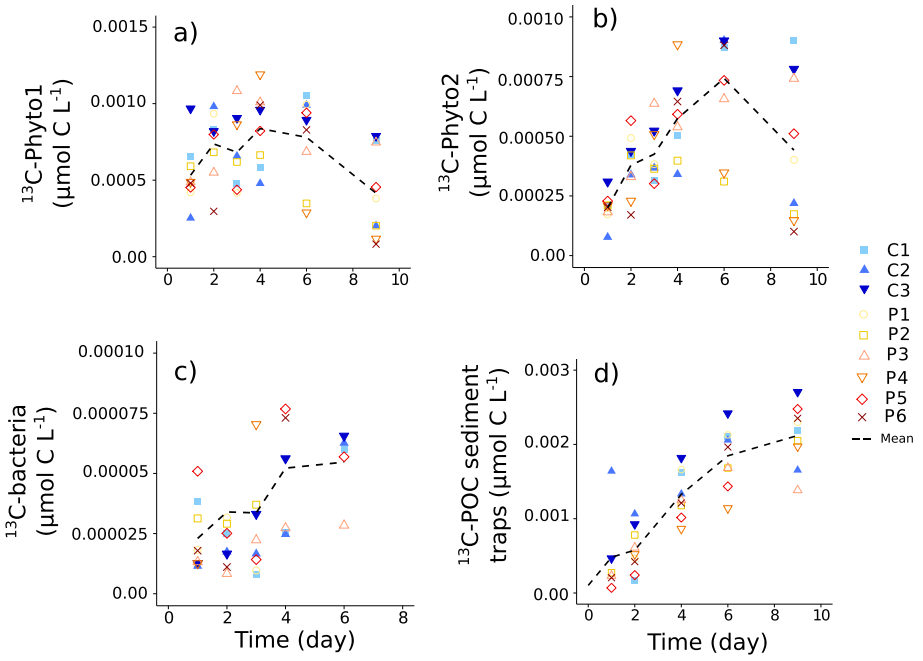

Fig. 6. ^{13}C-biomass (µmol ^{13}C L^{-1}) in the nine mesocosms (C1 to P6) deployed in the Bay of Villefranche in winter 2013 for a) fast-growing phytoplankton (Phyto1), b) slow-growing phytoplankton (Phyto2), c) heterotrophic bacteria and d) settling particles.

was already measured. ^{13}C-POC of settlings particles increased with time (Fig. 6d). The stepwise multiple regression analysis did show a negative effect of increasing pCO_2 (Table 2; $p < 0.001$) as well as relationships with most of the tested parameters. In contrast, cumulative ^{13}C-POC of settling particles varied independently of pCO_2 levels (linear regression on daily cumulative labelled material: $n = 9$, $r = -0.53$, $p > 0.05$).

3.4. Model results

Modelling was performed on biomass and ^{13}C labelling for both experiments. Due to the initial high ^{13}C-DIC labelling, the label in the DIC remained relatively constant, and global biomass did not significantly change in time (variability between replicates was much higher than through time) thus the model could be adequately applied. All compartments were well fitted except for ^{13}C-POC in BC suggesting that one phytoplankton group is missing to correctly model POC labelling. Growth rates are presented in Table 3 and were not significantly affected by elevated pCO_2 levels.

4. Discussion

The labelling studies showed a ^{13}C incorporation into pelagic particulate organic matter and different phytoplankton groups and subsequent transfer to heterotrophic bacteria and zooplankton as well as export to sediment traps despite environmental and sampling constrains. The ^{13}C incorporations in all compartments of the investigated plankton communities allowed for a qualitative and quantitative description of the dynamics of these communities and their potential dependence on CO_2.

Table 3
Modelled growth rates (d^{-1}) for the two phytoplankton groups (fast- and slow-growing phytoplankton groups, Phyto1 and 2, respectively) and heterotrophic bacteria, in the Bay of Calvi (summer 2012) and in the Bay of Villefranche (winter 2013).

Growth rate	Mean	±SD
Bay of Calvi		
Phyto1	0.38	0.03
Phyto2	0.16	0.01
Bacteria	0.14	0.01
Bay of Villefranche		
Phyto1	0.37	0.04
Phyto2	0.14	0.01
Bacteria	0.65	0.01

4.1. Environmental conditions and dynamics

The ^{13}C transfer from dissolved inorganic carbon to phytoplankton was evident for bulk organic matter, phytoplankton groups and heterotrophic bacteria in which significant labelling was measured after 1 or 2 days. Labelling was effective despite the low to extremely low phytoplankton biomasses, obtained with PLFA biomarkers (<0.2 µmol C L^{-1} in BC and <3 µmol C L^{-1} in BV). This is consistent with chlorophyll *a* concentrations that were low at both sites (<0.11 µg chl *a* L^{-1} in BC and <1.3 µg chl *a* L^{-1} in BV; see Gazeau et al., 2017b). In BC, the biomass of the phytoplankton group considered as slow-growing presented higher abundances than the fast-growing group while in BV, both groups contributed equally to phytoplankton biomass. Although heterotrophic bacterial abundances as estimated based on PLFA concentrations were difficult to obtain in BV, abundances during this winter experiment were higher than in summer in BC, consistently with flow cytometry cell counts (see Fig. S1; Celussi et al., 2017). Modelled heterotrophic bacterial growth rates were also much higher in BV than BC. With respect to production rates, net community production based on bulk ^{13}C incorporation (NCP-^{13}C) was higher in winter and decreased during the time of this experiment.

The plankton community in BC was characteristic of summer communities under nutrient-limited stratified conditions with a dominance of slow-growing phytoplankton, and based on regenerated production. This is supported by higher bacterial enzymatic activities measured in BC in summer than during the winter experiment (Celussi et al., 2017). In contrast, in winter, the fast-growing phytoplankton group presented higher production rates

than the slow-growing group at the start of the experiment, suggesting that the ecosystem was more at an autotrophic state. Toward the end of the experiment, the community tended to become more based on regenerated or secondary production as shown by the increase in regenerated nutrients (Louis et al., 2017) and decrease in the fast-growing phytoplankton group. During this winter experiment, theoretically conducted during the productive period in the Bay of Villefranche, nutrients were rapidly consumed during the first few days of deployment, leading to an unexpected N and P co-limitation at this period of the year and a shift from autotrophic to heterotrophic conditions. Final $\Delta\delta$-^{13}C ratios suggested that, during the summer experiment, a large inert organic compartment was present while in BV nearly all POC was ultimately labelled. Final $\Delta\delta$-^{13}C bacteria/$\Delta\delta$-^{13}C phytoplankton ratios was slightly higher in BC than in BV suggesting a stronger dependency of heterotrophic bacteria on phytoplankton derived carbon in summer and a fast turnover as compared to winter conditions. To summarize, while environmental and trophic conditions observed during the experiment in BC are fully representative of stratified unproductive conditions as observed in the Mediterranean Sea in summer, in winter, a fast nutrient consumption led to heterotrophic conditions that are not representative of this productive period. As such, extrapolation of results obtained during this deployment must be done with caution.

4.2. Methodological considerations

Although PLFA are useful to understand the functioning of a community or an ecosystem, particularly when combined with stable isotope analyses (Middelburg, 2014), the low daily sampling volume (~4 L due to necessary sampling restrictions) under these low nutrient concentrations and phytoplankton biomasses made the determination and quantification of PLFA rather difficult. Nevertheless, despite these methodological difficulties, ^{13}C incorporation was successfully traced through different phytoplankton groups and heterotrophic bacteria, showing an active carbon transfer between these compartments. It must be stressed that, in order to draw a full budget of carbon transfer in these communities, ^{13}C labelling of dissolved organic carbon (DOC) would have provided important information in these oligotrophic areas. However, ^{13}C-DOC in seawater remains very difficult to measure under high-labelled DIC concentrations. Furthermore, although PLFA are good taxonomic markers, most are shared by several phytoplankton groups and the PLFA composition of each species present in the studied community should be known to avoid misinterpretation (Zelles, 1999). In the Mediterranean Sea, few studies have been conducted on the attribution of PLFA to specific phytoplankton groups, therefore a conservative approach using a few broad phytoplankton groups, selected on incorporation patterns, was used to obtain group-specific information. The conversion factors, used to estimate carbon biomass from the measured PLFA concentrations, were based on data from phytoplankton strains sampled from estuaries, productive areas or nutrient-replete cultures. This has certainly introduced uncertainties in our estimates of biomass and production, but conversion factors are inevitable to quantitatively decipher carbon fluxes. Complementary laboratory studies should be performed to improve PLFA attribution to relevant phytoplankton groups of the Mediterranean Sea and to estimate proper conversion factors. Nevertheless, as identical conversion factors were used among mesocosms, this implies that they could not be responsible for the absence of CO_2 effects in our studies (see thereafter).

Finally, although mesocosms are often considered the experimental ecosystem closest to the "real world" (Riebesell et al., 2013), they are not exempt of complications due to local heterogeneity of plankton populations. While in summer in BC, starting conditions were rather homogeneous among mesocosms (see Fig. 2), a large variability between rates estimated in the three control mesocosms was observed during the more productive period in winter (see Fig. 6), most likely due to a stronger heterogeneity of plankton populations at that period of the year. This supports the choice of having several control treatments to characterize this natural variability. Finally, as already mentioned previously, during this experiment in winter, nutrients were rapidly consumed leading to unrepresentative conditions in mesocosms as observed to ambient conditions. It is out of the scope of this paper to discuss further these experimental uncertainties related to the use of mesocosms in dynamics and heterogeneous plankton communities.

4.3. Ocean acidification effect on carbon transfer

Net community production and phytoplankton group-specific production rates, biomasses based on PLFA as well as dependencies of consumers on resources obtained during the two experiments did not show any significant relationship with increasing pCO_2 levels. This is consistent with the other measurements of community production through bottle incubations (O_2 light–dark and ^{18}O, ^{14}C labelling; see Maugendre et al., 2017). The absence of pCO_2 effect on biomasses based on PLFA concentrations are also consistent with the resilience of plankton communities based on pigment and flow cytometry analyses (Gazeau et al., 2017b; Celussi et al., 2017). The zooplankton isotopic signature at the end of the experiment in BC did not show a significant pCO_2 effect although the highest CO_2 levels tended to have lower $\Delta\delta^{13}$C for both species collected. This tentatively suggests a reduced or delayed transfer of recently fixed carbon up the food web at the highest CO_2 levels (>1000 µatm), which is not foreseen until the end of the century. Freshly exported particulate matter was not sensitive to increased CO_2 levels in BC. This is coherent with the fact that no effect was measured on community and group-specific production rates. In contrast, labelling of settling particles in the Bay of Villefranche showed a significant decrease with increasing pCO_2. Considering that none of the other considered processes was significantly affected by an increase in pCO_2 and that cumulative labelling at the end of the experiment was not CO_2-dependent, a clear explanation of the nature of this negative effect over the course of the experiment could not be provided and has to be taken with caution.

To date, only one mesocosm experiment, conducted in high-latitude waters, followed the same ^{13}C enrichment protocol (De Kluijver et al., 2013). During this experiment in the Arctic (hereafter referred to as Svalbard), the effects of ocean acidification on production rates and carbon fluxes were subtle and depended on the growth phase considered (before or after nutrient addition; De Kluijver et al., 2013; Tanaka et al., 2013). During the first 12 days of the experiment (before nutrient addition), nutrient (nitrogen as nitrate and nitrite as well as phosphate) concentrations were close to or below detection limits of the conventional methods. This suggests very low levels and a dominance of slow-growing phytoplankton as during our summer experiment. Although chlorophyll *a* concentrations were similar between the experiments in BV and in Svalbard, POC concentrations were 2–3 times higher in Svalbard (~20–30 µmol L^{-1}; Schulz et al., 2013) than in BV (~10 µmol L^{-1}; Gazeau et al., 2017b). In all three experiments (BC, BV and Svalbard; Schulz et al., 2013; Gazeau et al., 2017b), phytoplankton communities were composed of small species such as haptophytes but communities differed by the presence of other small species such as cyanobacteria (mostly *Synechococcus* spp.) in BC and pelagophytes in BV that were absent or not reported as such in Svalbard where nano- and pico-phytoplankton were reported

(Brussaard et al., 2013). In Svalbard, although NCP-^{13}C did not change with increasing pCO_2, group-specific production rates of fast-growing and slow-growing phytoplankton tended to respectively increase and decrease as pCO_2 increased under nutrient-limited conditions (before nutrient addition). Therefore, despite similar chlorophyll *a* concentrations, the plankton community in Svalbard was more affected by elevated pCO_2 than during our experiments. It must be stressed that nutrient limitations were much stronger during our experiments, especially regarding PO_4^{3-} that remained 3 to 10 lower than levels measured in Svalbard at the start of this experiment.

While it appears evident that the response of plankton communities to ocean acidification depends on environmental conditions (e.g., nutrient levels), a recent study has highlighted the preponderant role of the community structure (Eggers et al., 2014). Phytoplankton species have several carbon concentration mechanisms (CCMs) that are species-dependent (e.g., Rost et al., 2008; Reinfelder, 2011). The initial ratio of diatoms, dinoflagellates and cyanobacteria could thus be responsible for large differences in the response to ocean acidification (Eggers et al., 2014). In contrast to laboratory results (Sala et al., 2015) on plankton communities from the Northwestern Mediterranean Sea, our experiments suggest that production and biomass of natural assemblages with large proportion of haptophytes, cyanobacteria (mostly *Synechococcus* spp.) and other small phytoplankton species will most likely be insensitive to ocean acidification.

The fact that no effect of ocean acidification was detected, in two experiments performed at two locations and seasons in the Northwestern Mediterranean Sea, for the great majority of measured parameters and processes, is very coherent considering the strong nutrient limitations observed during these experiments. As far as mesocosms can be considered as representative of natural conditions, our findings suggest that ocean acidification would have a limited effect on plankton communities structure and carbon transfer within pelagic compartments in oligotrophic areas for pCO_2 level expected by the end of the century. In addition, the different responses obtained between the two oceanic provinces that have been compared (Arctic *vs.* Mediterranean Sea) shows the need to consider a regional approach while studying the biological response to climate change (Häder et al., 2014). In fact, temperature, nutrient availability, plankton community composition and other unidentified parameters are major environmental and biological aspects that control the effect of human-induced perturbations such as ocean acidification. Finally, although some methodological improvements are still necessary, especially in oligotrophic unproductive areas, the use of ^{13}C enrichment combined with PLFA identification remains a very attractive method to estimate group-specific production rates and carbon transfer in mesocosms.

Acknowledgements

This work was funded by the EC FP7 project Mediterranean Sea Acidification in a changing climate (MedSeA; grant agreement 265103), the project European Free Ocean Carbon Enrichment (eFOCE; BNP-Paribas Foundation), the MISTRALS-MERMEX program (Institut des Sciences de l'Univers, INSU), the Corsican local authorities and the Rhone-Mediterranean and Corsica Water Agency. It is a contribution to the Surface Ocean – Lower Atmosphere Study (SOLAS) and Integrated Marine Biogeochemistry and Ecosystem Research (IMBER) projects and the Netherlands Earth System Science Center. The STARESO marine station in Corsica is gratefully acknowledged for its assistance and boat support carried out within the framework of the STARECAPMED project funded by the Rhone-Mediterranean and Corsica Water Agency. The staff of the Observatoire Océanologique de Villefranche is gratefully acknowledged for their assistance and boat support, colleagues of the Laboratoire d'Océanographie de Villefranche for providing laboratory space. Thanks are due to A. Sallon for organizing the experiments and logistics, F. Louis and J.-M. Grisoni for organizing the construction and deployment of the mesocosms as well as J.-M. Grisoni, A. Sallon, G. Obolensky, S. Alliouane, B. Hesse, D. Luquet, D. Robin, P. Mahacek and E. Cox for assistance with diving operations. Many thanks to M. Houtekamer, P. van Breugel and P. van Rijswijk for their advices and help in the laboratory for ^{13}C and PLFA analyses and Thierry Blasco for ^{13}C-POC analyses in Villefranche. L. Maugendre has been supported by a grant from the French Ministry of Higher Education and Research.

Appendix A. Supplementary data

Supplementary data related to this article can be found at http://dx.doi.org/10.1016/j.ecss.2015.12.018.

References

Adolf, J.E., Place, A.R., Stoecker, D.K., Harding, L.W., 2007. Modulation of polyunsaturated fatty acids in mixotrophic *Karlodinium* veneficum (Dinophyceae) and its prey, Storeatula major (Cryptophyceae) 1. J. Phycol. 43, 1259–1270.
Balzano, S., Pancost, R.D., Lloyd, J.R., Statham, P.J., 2011. Changes in fatty acid composition in degrading algal aggregates. Mar. Chem. 124, 2–13.
Boschker, H.T.S., Middelburg, J.J., 2002. Stable isotopes and biomarkers in microbial ecology. FEMS Microbiol. Ecol. 40, 85–95.
Brinis, A., Méjanelle, L., Momzikoff, A., Gondry, G., Fillaux, J., Point, V., Saliot, A., 2004. Phospholipid ester-linked fatty acids composition of size-fractionated particles at the top ocean surface. Org. Geochem. 35, 1275–1287.
Brussaard, C.P.D., Noordeloos, A.A.M., Witte, H., Collenteur, M.C.J., Schulz, K.G., Ludwig, A., Riebesell, U., 2013. Arctic microbial community dynamics influenced by elevated CO_2 levels. Biogeosciences 10, 719–731.
Celussi, M., Malfatti, F., Franzo, A., Gazeau, F., Giannakourou, A., Pitta, P., Tsiola, A., Del Negro, P., 2017. Ocean acidification effect on prokaryotic metabolism tested in two diverse trophic regimes in the Mediterranean Sea. Estuar. Coast. Shelf Sci. 186, 125–138.
Czerny, J., Schulz, K.G., Ludwig, A., Riebesell, U., 2013. A simple method for air/sea gas exchange measurement in mesocosms and its application in carbon budgeting. Biogeosciences 10, 1379–1390.
D'Ortenzio, F., D'Alcalà, M.R., 2009. On the trophic regimes of the Mediterranean Sea: a satellite analysis. Biogeosciences 6, 1–10.
Dalsgaard, J., John, M.S., Kattner, G., Muller-Navarra, D., Hagen, W., 2003. Fatty acid trophic markers in the pelagic marine environment. Adv. Mar. Biol. 46, 225–340.
De Kluijver, A., Soetaert, K., Czerny, J., Schulz, K.G., Boxhammer, T., Riebesell, U., Middelburg, J.J., 2013. A ^{13}C labelling study on carbon fluxes in Arctic plankton communities under elevated CO_2 levels. Biogeosciences 10, 1425–1440.
De Kluijver, A., Soetaert, K., Schulz, K.G., Riebesell, U., Bellerby, R.G.J., Middelburg, J.J., 2010. Phytoplankton-bacteria coupling under elevated CO_2 levels: a stable isotope labelling study. Biogeosciences 7, 3783–3797.
Dijkman, N., Boschker, H.T.S., Middelburg, J.J., Kromkamp, J.C., 2009. Group-specific primary production based on stable-isotope labeling of phospholipid-derived fatty acids. Limnol. Oceanogr. Methods 7.
Dijkman, N., Kromkamp, J.C., 2006. Phospholipid-derived fatty acids as chemotaxonomic markers for phytoplankton: application for inferring phytoplankton composition. Mar. Ecol. Prog. Ser. 324, 113–125.
Eggers, S.L., Lewandowska, A.M., Barcelos, E.R.J., Blanco-Ameijeiras, S., Gallo, F., Matthiessen, B., 2014. Community composition has greater impact on the functioning of marine phytoplankton communities than ocean acidification. Glob. Change Biol. 20, 713–723.
Engel, A., Delille, B., Jacquet, S., Riebesell, U., Rochelle-Newall, E., Terbrüggen, A., Zondervan, I., 2004. Transparent exopolymer particles and dissolved organic carbon production by *Emiliania huxleyi* exposed to different CO_2 concentrations: a mesocosm experiment. Aquat. Microb. Ecol. 34, 93–104.
Gazeau, F., Sallon, A., Lejeune, P., Gobert, S., Maugendre, L., Louis, J., Alliouane, S., Taillandier, V., Louis, F., Obolensky, G., Grisoni, J.M., Delissant, W., Guieu, C., 2017a. First mesocosm experiments to study the impacts of ocean acidification on the plankton communities in the NW Mediterranean Sea (MedSeA project). Estuar. Coast. Shelf Sci. 186, 11–29.
Gazeau, F., Sallon, A., Pitta, P., Pedrotti, M.L., Marro, S., Guieu, C., 2017b. Effect of ocean acidification on the plankton community diversity in the NW oligotrophic Mediterranean Sea: results from two mesocosm studies. Estuar. Coast. Shelf Sci. 186, 89–99.
Geri, P., El Yacoubi, S., Goyet, C., 2014. Forecast of sea surface acidification in the Northwestern Mediterranean Sea. J. Comput. Environ. Sci. 2014, 1–7.
Grossart, H.-P., Allgaier, M., Passow, U., Riebesell, U., 2006. Testing the effect of CO_2

concentration on the dynamics of marine heterotrophic bacterioplankton. Limnol. Oceanogr. 51, 1–11.
Häder, D.P., Helbling, W., Villafane, V., 2014. Productivity of aquatic primary producers under global climate change. Photochem. Photobiol. Sci. 13 (10), 1370–1392.
Hamilton, S.K., Tank, J.L., Raikow, D.F., Siler, E.R., Dorn, N.J., Leonardos, N.E., 2004. The role of instream *vs* allochthonous N in stream food webs: modeling the results of an isotope addition experiment. J. North Am. Benthol. Soc. 23, 429–448.
Kaneda, T., 1991. Iso-and anteiso-fatty acids in bacteria: biosynthesis, function, and taxonomic significance. Microbiol. Rev. 55, 288–302.
Klaas, C., Archer, D.E., 2002. Association of sinking organic matter with various types of mineral ballast in the deep sea: Implications for the rain ratio. Glob. Biogeochem. Cycles 16, 14–63.
Le Quéré, C., Peters, G.P., Andres, R.J., Andrew, R.M., Boden, T., Ciais, P., Friedlingstein, P., Houghton, R.A., Marland, G., Moriarty, R., Sitch, S., Tans, P., Arneth, A., Arvanitis, A., Bakker, D.C.E., Bopp, L., Canadell, J.G., Chini, L.P., Doney, S.C., Harper, A., Harris, I., House, J.I., Jain, A.K., Jones, S.D., Kato, E., Keeling, R.F., Klein Goldewijk, K., Körtzinger, A., Koven, C., Lefèvre, N., Omar, A., Ono, T., Park, G.-H., Pfeil, B., Poulter, B., Raupach, M.R., Regnier, P., Rödenbeck, C., Saito, S., Schwinger, J., Segschneider, J., Stocker, B.D., Tilbrook, B., van Heuven, S., Viovy, N., Wanninkhof, R., Wiltshire, A., Zaehle, S., Yue, C., 2014. Global carbon budget 2013. Earth Syst. Sci. Data 6, 235–263.
Longhurst, A., Sathyendranath, S., Platt, T., Caverhill, C., 1995. An estimate of global primary production in the ocean from satellite radiometer data. J. Plankton Res. 17, 1245–1271.
Louis, J., Guieu, C., Gazeau, F., 2017. Nutrient dynamics under different ocean acidification scenarios in a low nutrient low chlorophyll system: the Northwestern Mediterranean Sea. Estuar. Coast. Shelf Sci. 186, 30–44.
Maugendre, L., Gattuso, J.-P., Poulton, A.J., Dellisanti, W., Gaubert, M., Guieu, C., Gazeau, F., 2017. No detectable effect of ocean acidification on plankton metabolism in the NW oligotrophic Mediterranean Sea: results from two mesocosm studies. Estuar. Coast. Shelf Sci. 186, 89–99.
Middelburg, J.J., 2014. Stable isotopes dissect aquatic food webs from the top to the bottom. Biogeosciences 11, 2357–2371.
Middelburg, J.J., Barranguet, C., Boschker, H.T.S., Herman, P.M.J., Moens, T., Heip, C.H.R., 2000. The fate of intertidal microphytobenthos carbon: an *in situ* ^{13}C-labeling study. Limnol. Oceanogr. 45, 1224–1234.
Nielsen, L.T., Hallegraeff, G., Wright, S.W., Hansen, P.J., 2012. Effects of experimental seawater acidification on an estuarine plankton community. Aquat. Microb. Ecol. 65, 271–286.
Nielsen, L.T., Jakobse, H.H., Hansen, P.J., 2010. High resilience of two coastal plankton communities to twenty-first century seawater acidification: evidence from microcosm studies. Mar. Biol. Res. 6, 542–555.
Reinfelder, J.R., 2011. Carbon concentrating mechanisms in eukaryotic marine phytoplankton. Ann. Rev. Mar. Sci. 3, 291–315.
Riebesell, U., Schulz, K.G., Bellerby, R.G.J., Botro, M., Fritsche, P., Meyerhöfer, M., Neill, C., Nondal, G., Oschlies, A., Wohlers, J., Zöllner, E., 2007. Enhanced biological carbon consumption in a high CO_2 ocean. Nature 450, 545–548.
Riebesell, U., Bellerby, R.G.J., Grossart, H.-P., Thingstad, T.F., 2008. Mesocosm CO_2 perturbation studies: from organism to community level. Biogeosciences 5, 1157–1164.
Riebesell, U., Tortell, D., 2011. In: Gattuso, J.P., Hansson, L. (Eds.), Effects of Ocean Acidification on Pelagic Organisms and Ecosystems. Ocean Acidification, Cambridge, pp. 99–121.
Riebesell, U., Gattuso, J.P., Thingstad, T.F., Middelburg, J.J., 2013. Arctic ocean acidification: pelagic ecosystem and biogeochemical responses during a mesocosm study. Biogeosciences 10, 5619–5626.
Rivkin, R.B., Legendre, L., 2001. Biogenic carbon cycling in the upper ocean: effects of microbial respiration. Science 291.
Rossi, S., Sabatés, A., Latasa, M., Reyes, E., 2006. Lipid biomarkers and trophic linkages between phytoplankton, zooplankton and anchovy (*Engraulis encrasicolus*) larvae in the NW Mediterranean. J. Plankton Res. 28, 551–562.
Rost, B., Zondervan, I., Wolf-Gladrow, D.A., 2008. Sensitivity of phytoplankton to future changes in ocean carbonate chemistry: current knowledge, contradictions and research directions. Mar. Ecol. Prog. Ser. 373, 227–237.
Sala, M.M., Aparicio, F.L., Balague, V., Boras, J.A., Borrull, E., Cardelu, C., Cros, L., Gomes, A., Lopez-Sanz, A., Malits, A., Martinez, R.A., Mestre, M., Movilla, J., Sarmento, H., Vazquez-Dominguez, E., Vaqué, D., Pinhassi, J., Calbet, A., Calvo, E., Gasol, J.M., Pelejero, C., Marrase, C., 2015. Contrasting effects of ocean acidification on the microbial food web under different trophic conditions. ICES J. Mar. Sci. http://icesjms.oxfordjournals.org/content/early/2015/09/22/icesjms.fsv130.abstract?sid=c4d047d6-548d-469f-93a2-2a07d1ed11f3.
Schulz, K.G., Bellerby, R.G.J., Brussaard, C.P.D., Büdenbender, J., Czerny, J., Engel, A., Fischer, M., Koch-Klavsen, S., Krug, S. a., Lischka, S., Ludwig, A., Meyerhöfer, M., Nondal, G., Siljakova, A., Stuhr, A., Riebesell, U., 2013. Temporal biomass dynamics of an Arctic plankton bloom in response to increasing levels of atmospheric carbon dioxide. Biogeosciences 10, 161–180.
Soetaert, K., Petzoldt, T., 2010. Inverse modelling, sensitivity and Monte Carlo Analysis in R using package FME. J. Stat. Softw. 33.
Soetaert, K., Petzoldt, T., Woodrow Setzer, R., 2010. Solving differential equations in R: package deSolve. J. Stat. Softw. 33.
Taipale, S., Kankaala, P., Hämäläinen, H., Jones, R.I., 2009. Seasonal shifts in the diet of lake zooplankton revealed by phospholipid fatty acid analysis. Freshw. Biol. 54, 90–104.
Taipale, S., Strandberg, U., Peltomaa, E., Galloway, A., Ojala, A., Brett, M., 2013. Fatty acid composition as biomarkers of freshwater microalgae: analysis of 37 strains of microalgae in 22 genera and in seven classes. Aquat. Microb. Ecol. 71, 165–178.
Tanaka, T., Alliouane, S., Bellerby, R.G.J., Czerny, J., de Kluijver, A., Riebesell, U., Schulz, K.G., Siljakova, A., Gattuso, J.P., 2013. Effect of increased pCO_2 on the planktonic metabolic balance during a mesocosm experiment in an Arctic fjord. Biogeosciences 10, 315–325.
Tolosa, I., Vescovali, I., LeBlond, N., Marty, J.-C., de Mora, S., Prieur, L., 2004. Distribution of pigments and fatty acid biomarkers in particulate matter from the frontal structure of the Alboran Sea (SW Mediterranean Sea). Mar. Chem. 88, 103–125.
Tortell, P.D., DiTullio, G.R., Sigman, D.M., Morel, F.M.M., 2002. CO_2 effects on taxonomic composition and nutrient utilization in an Equatorial Pacific phytoplankton assemblage. Mar. Ecol. Prog. Ser. 236, 37–43.
Tortell, P.D., Payne, C.D., Li, Y., Trimborn, S., Rost, B., Smith, W.O., Riesselman, C., Dunbar, R.B., Sedwick, P., DiTullio, G.R., 2008. CO_2 sensitivity of Southern Ocean phytoplankton. Geophys. Res. Lett. 35, L04605.
Touratier, F., Goyet, C., 2009. Decadal evolution of anthropogenic CO_2 in the Northwestern Mediterranean Sea from the mid-1990s to the mid-2000s. Deep. Res. 56, 1708–1716.
Van den Meersche, K., Middelburg, J.J., Soetaert, K., van Rijswijk, P., Boschker, H.T.S., Heip, C.H.R., 2004. Carbon-nitrogen coupling and algal-bacterial interactions during an experimental bloom: modeling a ^{13}C tracer experiment. Limnol. Oceanogr. 49, 862–878.
Van den Meersche, K., Soetaert, K., Middelburg, J.J., 2011. Plankton dynamics in an estuarine plume: a mesocosm ^{13}C and ^{15}N tracer study. Mar. Ecol. Prog. Ser. 429, 29–43.
Van Oevelen, D., Moodley, L., Soetaert, K., Middelburg, J.J., 2006. The trophic significance of bacterial carbon in a marine intertidal sediment: results of an *in situ* stable isotope labeling study. Limnol. Oceanogr. 51, 2349–2359.
Viso, A.C., Marty, J.C., 1993. Fatty acids from 28 marine microalgae. Phytochemistry 34.
Zelles, L., 1999. Fatty acid patterns of phospholipids and lipopolysaccharides in the characterisation of microbial communities in soil: a review. Biol. Fertil. Soils 29, 111–129.